Rock Mech. Rock Engng. (2003) 36 (1), 3–25
DOI 10.1007/s00603-002-0033-1

Rock Mechanics and Rock Engineering
Printed in Austria

A New Method for In-situ Non-contact Roughness Measurement of Large Rock Fracture Surfaces

By

Q. Feng, N. Fardin, L. Jing, and **O. Stephansson**

Engineering Geology and Geophysics Research Group, Department of Land and Water Resources Engineering, Royal Institute of Technology, Stockholm, Sweden

Received May 24, 2001; accepted July 24, 2002;
Published online November 19, 2002

Summary

This paper presents a new method for in-situ non-contact measurements of fracture roughness by using a total station (TS). The TS is a non-reflector geodetic instrument usually used for measuring control points in surveying and mapping. By using a special-developed program, the TS can be used as a point-sensor laser scanner to scan a defined area of the fracture surface automatically, in field or in laboratory, at a distance away from the target surface. A large fracture surface can be automatically scanned with a constant interval of the sampling points, both within a defined area or along a cross-section of the exposed rock face. To quantify fracture roughness at different scales and obtain different densities of the scanned points, the point interval can be selected with the minimum interval of 1 mm. A local Cartesian co-ordinate system needs to be established first by the TS in front of the target rock face to define the true North or link the measurements to a known spatial co-ordinate system for both quantitative and spatial analysis of fracture roughness. To validate the method, fracture roughness data recorded with a non-reflector TS was compared with the data captured by a high-accuracy 3D-laser scanner. Results of this study revealed that both primary roughness and waviness of fracture surfaces can be quantified by the TS in the same accuracy level as that of the high accuracy laser scanner. Roughness of a natural fracture surface can be sampled without physical contact in a maximum distance of tens of meters from the rock faces.

Keywords: Roughness, waviness, primary roughness, fracture surface, geodetic non-reflector total station, laser scanning, large fracture surface, in-situ measurement.

1. Introduction

Fracture roughness is mostly characterized in laboratory on small specimens of natural fracture surfaces. However, in-situ measurement and determination of fracture roughness at large-scale is very important to understand and quantify the effect of scale on fracture roughness, which has the significant impact on defor-

mation of rock masses and hydro-mechanical behavior of fractured rocks. The characterization of fracture surface geometry is currently one of the most active research fields in rock engineering.

Several methods have been proposed in the literatures for quantification of fracture roughness, e.g. the Joint Roughness Coefficient (Barton et al., 1977), various statistical parameters (Piggott et al., 1995; Roko et al., 1997) and the fractal theory (Odling, 1994; Xie, 1993). However, the applicability and the reliability of the fracture roughness analysis highly depend on the method and the accuracy of the data acquisition. Current technology for sampling of fracture surfaces can be categorized as contact and non-contact approaches, ranging from simple manual methods to mechanical profiling methods, and highly sophisticated automatic optical methods. The contacting approach requires the operator or instrument to physically contact the surface for recording the measurements along the chosen profiles or over the defined area. For instance,

- the linear profiling method (Fecker et al., 1971; Weissbach, 1978);
- the compass and disc-clinometer method (Fecker et al., 1971);
- the shadow profilometry method (Maerz et al., 1990);
- the tangent plane sampling and the connected pin sampling techniques introduced by Rasouli et al. (2000);
- and the well-known mechanical or electronic stylus profilometers.

These methods have some drawbacks, as they are time-consuming for capturing the measurements and insufficient data recording at dangerous and inaccessible locations.

The non-contact approach employs a technique to capture the measurements without physically touching fracture surfaces, as demonstrated by:

- the analytical photogrammetry method (Wickens et al., 1971);
- the electro-fiber-optic system (Yilbas et al., 1987);
- the image processing method (Galante et al., 1991);
- the interferometry method (Shukla et al., 1991);
- the fibre-optic probe and He-Ne laser beam technique (Yilbas et al., 1998);
- the laser scanning method (Lanaro et al., 1998);
- and the advanced topometric sensor (ATS) technique (Grasselli et al., 2000).

These methods greatly improved the speed and accuracy of roughness measurements. However, many of these methods can only be used in the laboratory for measuring small specimens within a close range of measuring distances. Especially, the data collected by these methods can not be applied for spatial analysis of fracture roughness in the real space, e.g. roughness features at a special direction and location of the exposed fracture surface, which is important for design and characterization purposes in rock engineering.

The total station (TS) is a non-reflector geodetic instrument, which is usually used for measuring the co-ordinates of control points in space (Moffitt et al., 1998). It has also been applied in rock engineering for determining fracture traces on inaccessible rock slopes (Bulut et al., 1996), and for measuring dip angle and dip direction of fractures on exposed rock faces (Feng et al., 2001). Because a laser

beam is used, the non-reflector TS can record the position without putting any reflector at the target, and the target itself reflects back the signal. By using a special program, the non-reflector TS can be used as a point-sensor laser scanner to capture co-ordinates of a large number of target points automatically within a defined area. Therefore, the TS provides an alternative for *in-situ* sampling of fracture surfaces and allows for spatial analysis of fracture roughness in a known spatial co-ordinate system within a distance of tens of meters. A selected area or some profiles on the fracture surface can be automatically scanned with a adjustable interval between the measuring points. The interval can be adjusted for different densities of the scanned points and different scales.

The objective of this paper is to present the TS measuring principle and sampling procedure for in-situ roughness measurements. The measurement accuracy of the presented method was tested and compared with a high-accuracy 3D-laser scanner method. Characterization of the roughness of a large fracture surface based on the measurements is also presented.

2. Methodology

2.1 Non-reflector Geodetic Total Station

The geodetic total station first appeared in the late 1980s as a result of the development of electronics and computerization of surveying instrumentations (Kavanagh et al., 1992). With the rapid development of electronics and computer technology in the 1990s, the TS is now undergoing a rapid refinement of its functions, accuracy and lowering of the cost. Although the TS was designed for geodetic survey, it is also applied in rock engineering for fracture mapping at exposed rock faces (Bulut et al., 1996; Feng et al., 2001). The new functions (e.g. scanning in a defined area) of the non-reflector TS are also useful for characterization of fracture roughness.

The TS is essentially an electronic theodolite that contains an integral electronic distance measurement unit (EDM) with coaxial optics. The typical TS instrument consists of four main components: i) an EDM; ii) an electronic theodolite (ET); iii) a data collector; and iv) an on-board microprocessor (Moffitt et al., 1998).

Figure 1 schematically shows the measuring principle of the TS. The EDM is used to measure the slope distance of a target point P. The ET measures the horizontal and vertical angles from the TS to a target. From the measurements of angles and distances, the co-ordinates of the target point are calculated with Eq. (1) by the on-board microprocessor.

$$\left\{ \begin{array}{l} X = S\cos(VA)\cos(HA) \\ Y = S\cos(VA)\sin(HA) \\ Z = S\sin(VA) \end{array} \right\} \tag{1}$$

where S = Slope distance, VA = Vertical Angle, HA = Horizontal Angle.

The results are stored in the data collector. These raw data can be transferred to a computer for any surveying-related application.

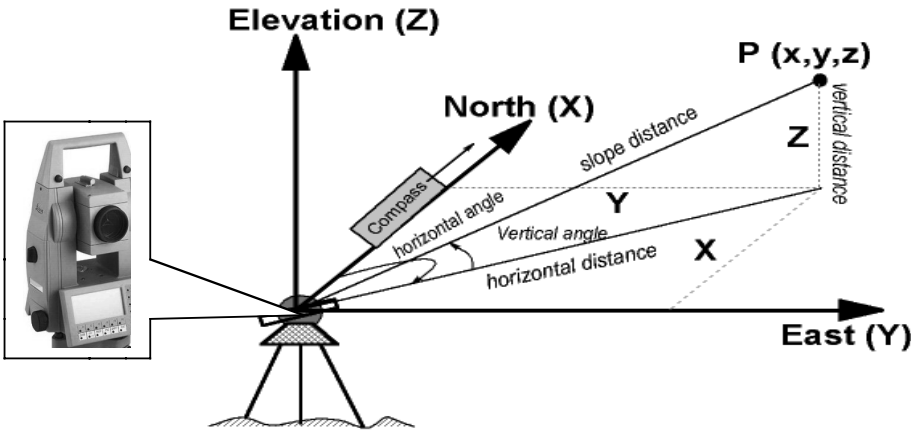

Fig. 1. Definition of co-ordinates of a point within a local co-ordinate system

The TS instruments can be categorized in two types, i.e. the reflector TS and the non-reflector TS, according to the measuring principle of the EDM. Current EDMs use either infrared light (light waves) or microwaves (radio waves). The microwave EDMs require a transmitter/receiver at both ends of the measured line, whereas the infrared EDMs require a transmitter at one end and a reflecting prism at the other end. A recently developed EDMs can measure distances without using reflecting prisms. These EDMs employ a timed-pulse infrared signal transmitted by a laser diode to permit direct acquisition of distances from the target by using the target surface itself as a reflector. Currently, many TS instruments on the market use the infrared EDM, and can switch between reflector and non-reflector modes.

2.2 Scanning Principle by a Non-reflector Geodetic Total Station

The non-reflector TS is useful to measure fracture roughness in a non-contacting approach. In general, the TS measures the target points one by one through a sequential procedure of aiming, capturing and recording, which is manually controlled by the operator. If a special-developed program is used, the non-reflector TS can automatically execute the whole measuring procedure and capture the target points (SBG, 1999; Leica, 1999). In this case, the non-reflector TS can be taken as a point-sensor laser scanner to scan a selected part of a fracture surface or any objects.

To scan a fracture surface in the field, a typical scanning procedure consists of the following three main steps:

1. Establishing a 3-D Cartesian co-ordinate system

A Cartesian co-ordinate system must be established in order to quantify the fracture roughness in a reference co-ordinate system. Depending upon the requirements of different applications, the TS can be used to set up three types of the reference co-ordinate systems:

– i) If only the relative positions between the TS and the target points are required, a local Cartesian co-ordinate system can be easily set up by the TS itself. The origin can be settled at the location of the TS instrument.
– ii) If true North must be known in the local co-ordinate system, a compass is needed. The setting procedure is similar to those of the first method. The positive X-axis coincides with true North (see Fig. 1).
– iii) If the control points accessing to GPS (Global Positioning System) are available, the local Cartesian co-ordinate system can be linked to a global reference system, e.g. national ground co-ordinate system, global geographical co-ordinate system. This might be useful if the spatial analysis of fracture roughness is required.

2. Defining a scanning area

Before performing the automatic scanning of a fracture surface, a target area on the fracture surface as well as the interval between adjacent points must be defined. The scanning program allows the operator to input some parameters to select a scanning region on the fracture surface and define an interval of the adjacent points to be recorded. Then, the TS can automatically measure the target points within the selected area at a constant interval. In this study, the scanning program, Leica TMS PROscan version 1.0 (Leica, 1999), was used. Figure 2 schematically shows the scanning principle of this program. To select a scanning area, four corner points, e.g. P1, P2, P3 and P4, of an area must be measured in a sequence from the upper left P1 to the upper right P2, and then to the lower right P4 until the lower left P3. The interval along the X-direction (P1–P2) and the Y-direction (P1–P3) can be set up respectively, with the minimum distance of 1 mm.

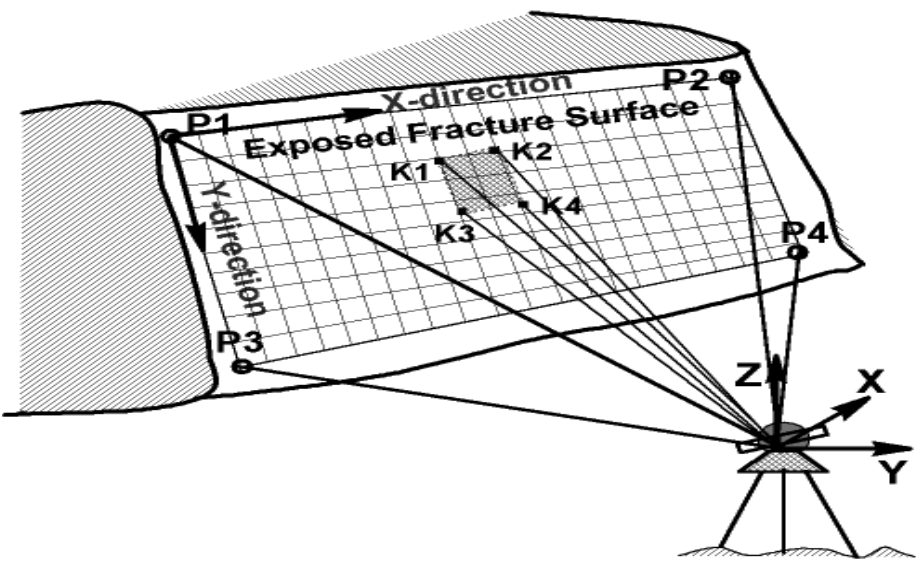

Fig. 2. Automatic scanning of a fracture surface by a non-reflector TS

The interval in the X-direction can be chosen either with the same value as the one for the Y-direction to achieve a constant point density within the whole scanning area, or the interval can be set with different values along the two directions. By using this program, both an area and a profile on a fracture surface can be automatically scanned.

3. Scanning and recording
After selecting both the target area and the point interval, the TS will automatically scan the fracture surface, point by point, along each scan-line. During the scanning, the position of the scanned points is continuously computed by the scanning program in the following ways:

– i) Number of scan lines $= \dfrac{(\text{Distance of (P1–P3)} + \text{Distance of (P2–P4)})/2}{\text{Y-direction interval}}$;
– ii) For each scan-line, the points are distributed so that the defined interval in the X-direction is achieved as good as possible.

The TS can stand tens of meters away from the surface to scan. A large size of the fracture surface can be scanned, and the maximum scanning area depends upon the position and the viewing range of the TS. The time for the procedure of aiming, capturing and recording the data for each point takes about 3 seconds if the TS is standing within 30 meters from the fracture surface. The scanning data are stored dynamically in a memory card inside the TS and can be downloaded to a computer for further analyses.

2.3 Data Processing for Surface Roughness Analysis

The co-ordinates of the scanned points recorded by the TS can be transferred to a computer, and then input to the programs for quantitative and spatial analysis of fracture roughness. In this study, a commercial software, Surfacer version 10.0 (Imageware, Inc., 1999) and several special programs developed in C/C++ and MatLab are used for data transformation, calculation of roughness parameters, spatial analysis of roughness along different directions etc.

3. Accuracy of the TS

Since the TS is an integrated instrument containing an electronic distance measurement device (EDM) and an electronic theodolite (ET), the accuracy of TS measurements depends upon both the EDM and the ET. The non-reflector TS used in this study, Leica TCRM 1102, has the resolution of $1''$ and the accuracy of $2''$ for the ET, and its EDM has the resolution of 1 mm and the accuracy of 3 mm $\pm$ 2 ppm (Leica, 1998).

When using the TS for fracture mapping, the co-ordinates of the target points are used as raw data for computing fracture roughness. Therefore, it is important to notice how accurate the co-ordinates of a target point can be measured by the TS. However, if just reading the information from the manual of a TS instrument, it is not clear enough for geologists and geotechnical engineers to understand the

accuracy of the TS measurements. There are two main reasons: i) the TS manual only presents the resolution and accuracy of the distance measurements by the EDM and the angular measurements by the ET, respectively. The accuracy of the co-ordinate measurements depends on the distance and angular measurements. ii) the specified accuracy is usually obtained in the standard mapping conditions, and may change in non-standard conditions. For example, the standard condition is that the emitted light or laser beam should be nearly perpendicular to the target surface, and the target surface should be flat and smooth. But when measuring a rock face, the mapping conditions are usually far from being standard due to several influential factors, e.g. roughness of the fracture surface, inclination angle from the emitted light onto the rock faces. Therefore, the errors originate from two main sources: i) instrument-related errors; and ii) surface-related errors.

To provide a clear idea about the accuracy of the TS measurements, the error analysis theory can be applied to estimate the accuracy of the point co-ordinates from the measurements of the EDM and the ET. A special test was conducted in this study to investigate the influence of rock faces and fracture surfaces on the TS measurements.

Since the co-ordinates of a target point are computed from Eq. (1), the propagated errors (dE) on the co-ordinates (X, Y, Z) of a point P can be derived as follows (Fan, 1997):

$$dE = \begin{bmatrix} dX \\ dY \\ dZ \end{bmatrix} = \begin{bmatrix} \frac{\partial X}{\partial S} & \frac{\partial X}{\partial \theta_V} & \frac{\partial X}{\partial \theta_H} \\ \frac{\partial Y}{\partial S} & \frac{\partial Y}{\partial \theta_V} & \frac{\partial Y}{\partial \theta_H} \\ \frac{\partial Z}{\partial S} & \frac{\partial Z}{\partial \theta_V} & \frac{\partial Z}{\partial \theta_H} \end{bmatrix} \begin{bmatrix} \varepsilon_S \\ \varepsilon_{\theta_V} \\ \varepsilon_{\theta_H} \end{bmatrix} = \begin{bmatrix} \frac{\partial X}{\partial S}\varepsilon_S + \frac{\partial X}{\partial \theta_V}\varepsilon_{\theta_V} + \frac{\partial X}{\partial \theta_H}\varepsilon_{\theta_H} \\ \frac{\partial Y}{\partial S}\varepsilon_S + \frac{\partial Y}{\partial \theta_V}\varepsilon_{\theta_V} + \frac{\partial Y}{\partial \theta_H}\varepsilon_{\theta_H} \\ \frac{\partial Z}{\partial S}\varepsilon_S + \frac{\partial Z}{\partial \theta_V}\varepsilon_{\theta_V} + \frac{\partial Z}{\partial \theta_H}\varepsilon_{\theta_H} \end{bmatrix} \quad (2)$$

where S is the slope distance, θ_V is the vertical angle, θ_H is the horizontal angle; the error of the co-ordinates of a point P(X, Y, Z) are dX, dY, dZ; $\varepsilon_S, \varepsilon_{\theta_V}, \varepsilon_{\theta_H}$ are errors of the slope distance measurements from the EDM, and the vertical and horizontal angle measurements from the ET, respectively. The partial differential elements in Eq. (2) can be determined by:

$$\frac{\partial X}{\partial S} = \cos\theta_V \sin\theta_H, \quad \frac{\partial X}{\partial \theta_V} = -S\sin\theta_V \sin\theta_H, \quad \frac{\partial X}{\partial \theta_H} = S\cos\theta_V \cos\theta_H;$$

$$\frac{\partial Y}{\partial S} = \cos\theta_V \cos\theta_H, \quad \frac{\partial Y}{\partial \theta_V} = -S\sin\theta_V \sin\theta_H, \quad \frac{\partial Y}{\partial \theta_H} = -S\cos\theta_V \sin\theta_H;$$

$$\frac{\partial Z}{\partial S} = \sin\theta_V, \quad \frac{\partial Z}{\partial \theta_V} = S\cos\theta_V, \quad \frac{\partial Z}{\partial \theta_H} = 0$$

Therefore, the accuracy of the point co-ordinates depends on the accuracy of both distance and angle measurements.

When measuring the target points on a fracture surface, factors such as roughness of and reflectance of the surface and inclination angle from the laser beam to the surface, influence the accuracy of co-ordinate measurements of the

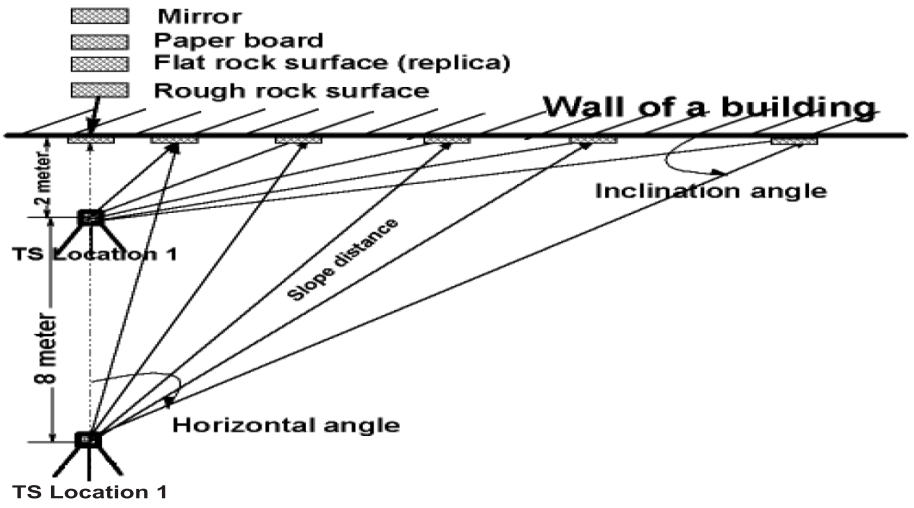

Fig. 3. Accuracy test for the surface-related influential factors

target points. These errors are of special concern when measuring the targets on rock surfaces, and are called surface-related errors in this paper. To check the influence of the surface-related errors, a test study was performed. In this test, four factors are considered: i) inclination angle, i.e. the angle between the laser beam and the surface; ii) roughness of the surface; iii) reflectance of the surface and iv) distance from the TS location to the targets.

Figure 3 schematically shows the test procedure. A vertical wall of a building facing to true North was selected as a base plane. A non-reflector TS (Leica TCRM 1102) was standing at two locations (see Fig. 3), i.e. Location 1 and Location 2 with a normal distance to the wall of about 2 m and 8 m, respectively. Small samples of four types of the material surfaces are chosen: i) a mirror surface; ii) a paperboard surface; iii) a silicon rubber replica surface of a flat rock fracture surface and iv) a sample of a rough rock fracture surface. These samples represent the fracture surfaces with different roughness and reflectance properties, and were put at different positions on the base plane. By the guidance of the ET, these samples were positioned along an almost horizontal band on the base plane. By adjusting the ET to make the vertical and the horizontal angle as zero degree, the laser beam was shooting perpendicularly onto the sample surface. Then, the horizontal angle was increased in order to decrease the inclination angle while keeping the vertical angle at zero degree. The influence of both inclination angle and slope distance can be detected. On each sample surface, a 8 cm segment was marked and pre-measured by a ruler with the accuracy of 0.5 mm, and also measured by the TS. Once the co-ordinates of the two end points of the segment were recorded by the TS, the length of the segment was calculated and compared with the known length. Figures 4, 5 show the results of the test. The diagrams show the deviation (the X-axis), between the known length of the segment and the one measured by the TS, is changed with the inclination angle (the left-side Y-axis) and the slope

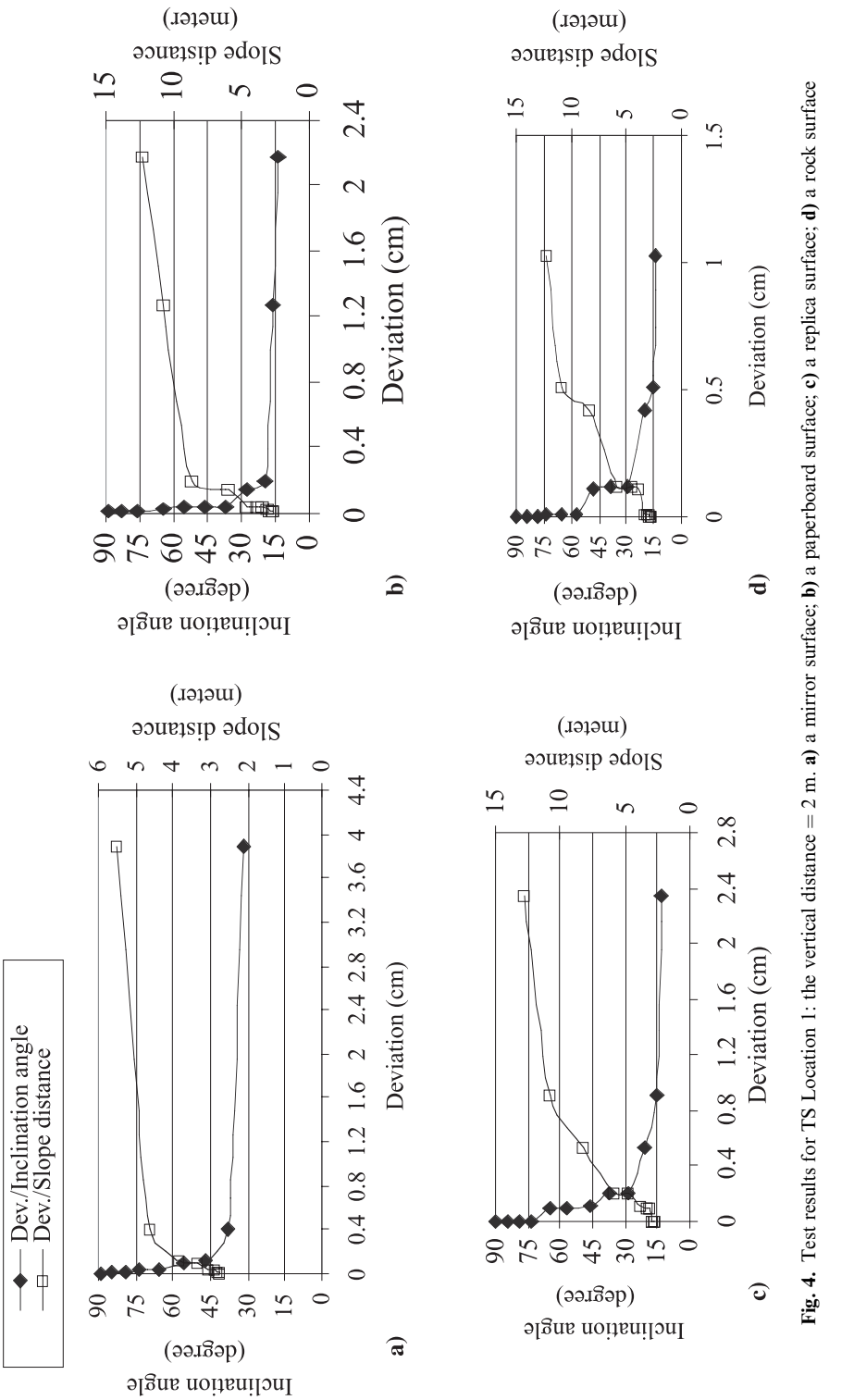

Fig. 4. Test results for TS Location 1: the vertical distance = 2 m. **a)** a mirror surface; **b)** a paperboard surface; **c)** a replica surface; **d)** a rock surface

distance (the right-side Y-axis). The results indicate that the deviation is affected by the above-mentioned four influential factors. When decreasing inclination angles, the deviation is increased. Meanwhile, the deviation increases when increasing the slope distance. It seems that there is a threshold for the inclination angle, and different types of the surfaces have different threshold inclination angles. For the mirror surface, the threshold angle is much larger than other surfaces. For the surfaces with different amplitudes of roughness, the deviation changes. The rougher the surface the bigger the deviation. The above-mentioned four factors also influence each other. If the vertical distance is increased, the threshold inclination angle for these surfaces is decreased (Fig. 5). Therefore, the surface-related errors must be considered when measuring targets on the rock faces by the TS.

4. Comparing TS and 3D Laser Scanner Results

To check the accuracy of roughness measurements by using TS, a replica of a fracture surface was scanned in the laboratory by using both the TS and a high-accuracy 3D-laser scanner. The replica was made of silicon rubber and represents a part of a natural fracture surface with a size of 120 mm $\times$ 120 mm. A high-accuracy 3D-laser scanner has been used for the laboratory study of the roughness of rock fracture surfaces (Lanaro et al., 1998; Fardin et al., 2001). It is a strip-sensor laser scanner, which means the laser beam projects a strip of 25 mm wide on the object surface and scans the object surface strip by strip. Each strip contains 600 points with 50 μm interval. The accuracy of this laser scanner is high up to $\pm$20 μm with the resolution of 10 μm. The laser can scan a sample with a maximum dimension of 1000 mm $\times$ 1040 mm $\times$ 420 mm. Detailed features of this scanner are described in (Lanaro et al., 1998).

For this test, the interval of the scanning points was kept as 5 mm for the two scanning methods in order to characterize the surface roughness with the same density of the sampling points. The digital topographical models from both methods of the replica are shown in Fig. 6. They are slightly different because of the lower resolution for the TS method, but the overall roughness features of the surface are similar.

4.1 Methods for Surface Roughness Characterization

In the literature, many different methods have been suggested for characterization of the rock joint surface roughness. The fractal theory (Mandelbrot, 1967, 1983) was used in this study for analysis of the surface roughness. At least two parameters are required to characterize a self-affine fractal object: 1) the fractal dimension D, which describes how roughness changes with scale; 2) the amplitude parameter A, which specifies the variance or surface slope at a reference scale. The autocorrelation structure of a surface is captured by the fractal dimension D, or Hurst exponent H ($0 < H < 1$). The parameters H and D are related by the equation $H = E - D$, where E is the Euclidean dimension ($E = 3$ for a surface and $E = 2$

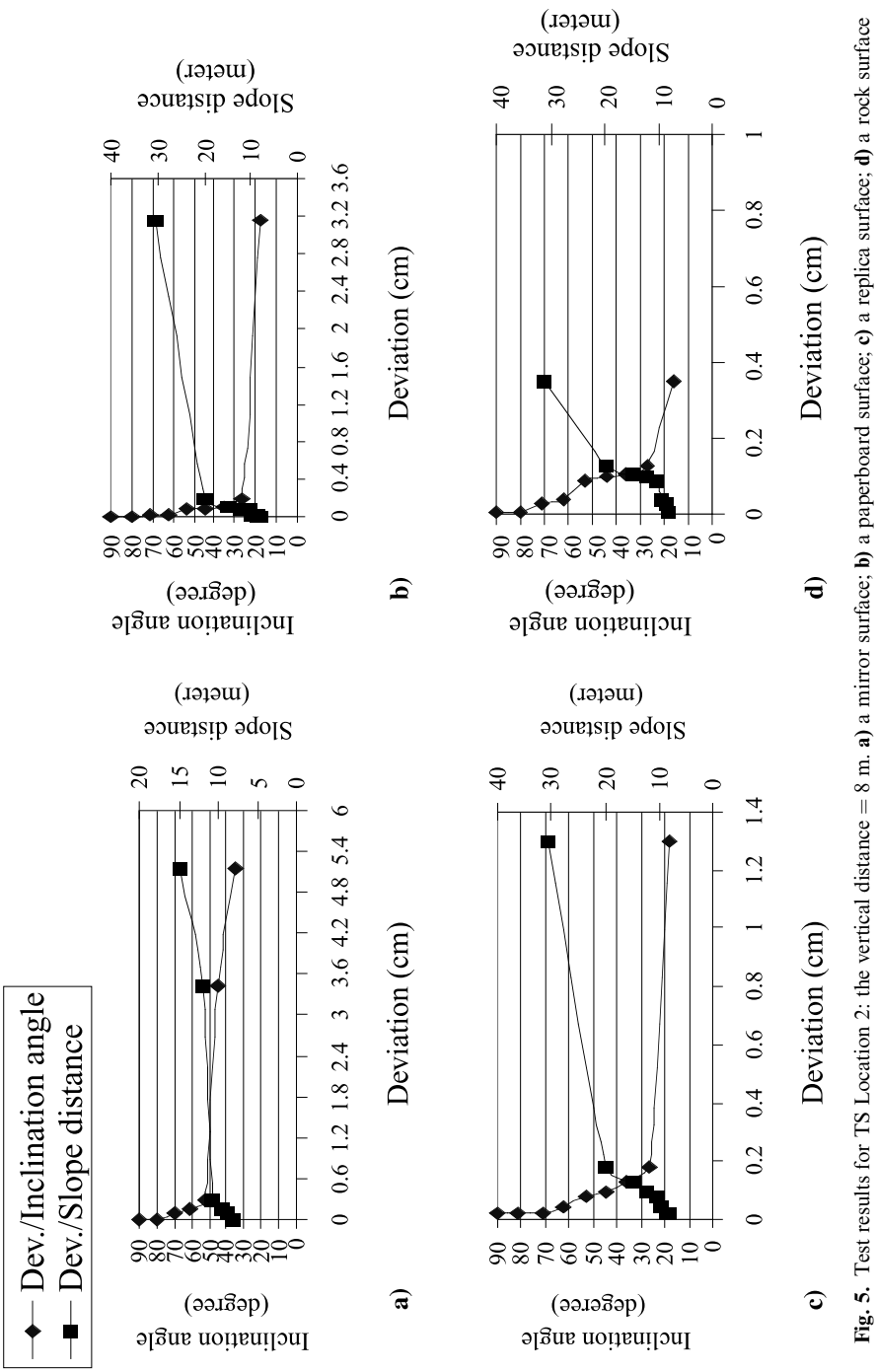

Fig. 5. Test results for TS Location 2: the vertical distance = 8 m. **a)** a mirror surface; **b)** a paperboard surface; **c)** a replica surface; **d)** a rock surface

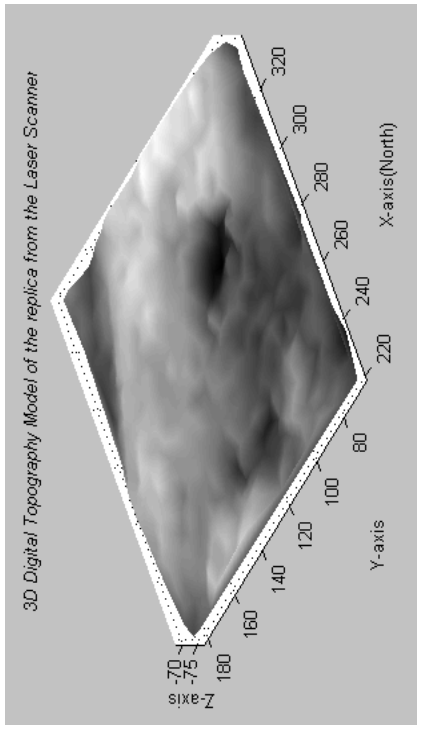

(a) **(b)**

Fig. 6. 3-D digital topographical models of the replica created by the TS **(a)** and the laser scanner **(b)**

for a profile) for a self-affine fractal object. Both the auto-correlation (i.e. H or D) and amplitude (A) of a surface contribute to the roughness of the surface. To estimate D and A, several methods have been introduced in the literatures, such as the variogram method (Orey, 1970), the structure function (SF) method (Sayles et al., 1977), the spectral method (Berry et al., 1980), the Roughness-Length (RL) (Malinverno, 1990) and the line scaling method (Matsushita et al., 1989). In this study, the fractal parameters D and A, are calculated with both the RL and SF methods.

4.1.1 Roughness-Length (RL) Method

For a self-affine fractal profile, there is a power law relation between the standard deviation of the profile heights $S(w)$ and sampling window length of the profile w as follows (Malinverno, 1990):

$$S(w) = Aw^H, \tag{3}$$

where H and A are the Hurst exponent and a proportionality constant, respectively. The proportionality constant A is defined as a measure of amplitude of a profile (amplitude parameter). $S(w)$ is calculated as the root-mean-square value of the profile height residuals on a linear trend fitted to the sample points in a window of length w. If a log-log plot of $S(w)$ versus w gives an acceptably straight line, the parameters H and A can be easily estimated as the slope and intercept of the obtained line respectively, as shown in Fig. 7.

The above methodology was derived for calculating fractal parameters of the roughness of the replica by using Eq. (3). A power law relation between the standard deviation of the residual surface heights $S(w)$ and sampling window size w is defined for a self-affine surface, in the same form as Eq. (3). To calculate the fractal parameters, the replica surface is divided into a grid of squares of desired window size (w). For each square, a local interpolation plane is defined by a least-squares regression analysis (Fig. 8). The residuals of the asperity height, defined as the normal distance between the surface asperity heights and their local interpolation plane and $S(w)$ are then calculated for each square through a special program written in the Surfacer Imageware code.

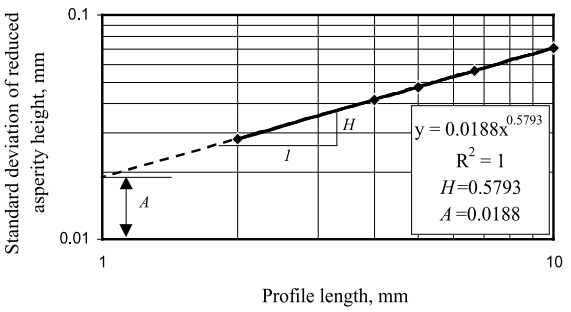

Fig. 7. Log-log plot of the standard deviation of the reduced asperity height versus profile length of the replica (after Fardin et al., 2001)

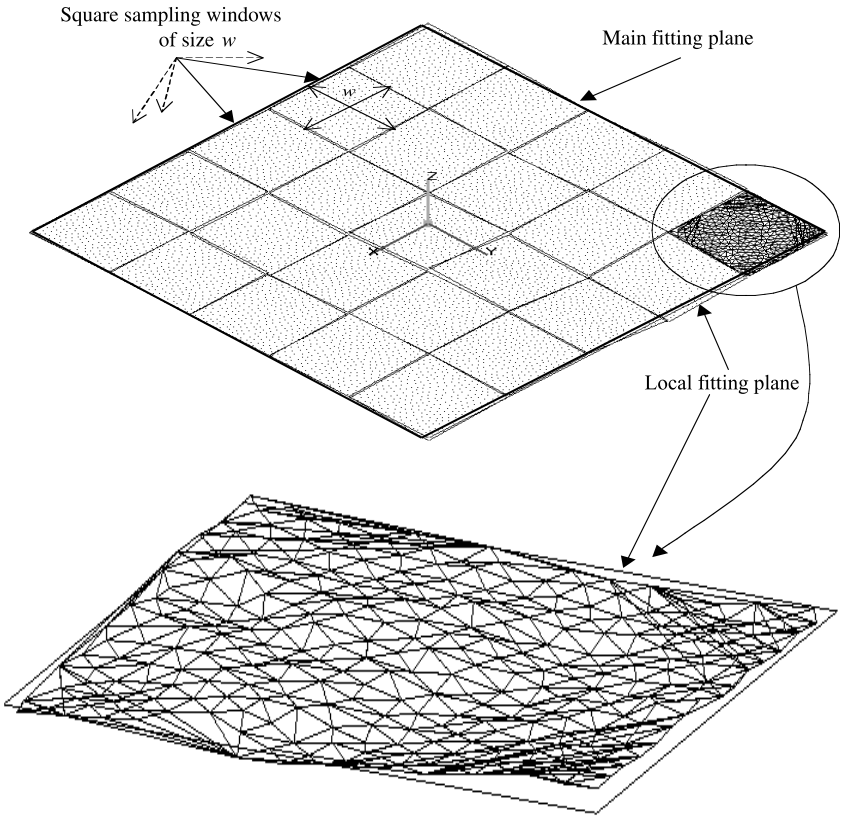

Fig. 8. The main and local fitting planes, grid of squares of sampling windows of size w and a triangularization of local surface of a sampling window (after Fardin et al., 2001)

4.1.2 Structure Function (SF) Method

The structure function, $SF(x)$, is simply the mean square height difference of points on the profile at horizontal separations of x. For a range of measure intervals, $SF(x)$ is defined as (Odling, 1994):

$$SF(x) = (Y(X + x) - Y(X))^2. \tag{4}$$

The structure function $SF(x)$ is also related to the Hurst exponent H (Voss, 1988; Poon et al., 1992):

$$SF(x) = Ax^{2H}. \tag{5}$$

Therefore, if a log-log plot of $SF(x)$ versus x gives an acceptable straight line, the slope of this line gives $2H$. A is also defined as an amplitude parameter and is equivalent to the mean square height difference at a measure interval of 1 unit, and is therefore dependent on the units of measurement. In the above equations, when

w or x are equal to 1, it follows that $S(w) = A$. As different units (e.g. mm, cm, m, km) can be used to represent w, different A values are possible for the same surface depending on the unit used for w. It means that the scale effect for roughness of rock joints can be captured by this amplitude parameter A.

4.2 Results

Using the above-mentioned methods, the roughness of the replica surface was quantified. First of all, the whole surface of the replica was analyzed by using the RL method. To calculate the fractal parameters D and A, the surface was divided into a number of sets of sub-windows (see Fig. 8). Each set of sub-windows has the window size w of 20 mm, 24 mm, 30 mm, 40 mm and 60 mm, respectively. Then, the standard deviations of the reduced asperity height $S(w)$ was calculated for all sets of sub-windows with the window size w. The calculated mean values of $S(w)$ of the replica surface are plotted against their sub-window size w in the log-log diagram (see Fig. 9). As shown in Fig. 9, a very good linear relation exists between $S(w)$ and w for both digitized surfaces. The fractal parameters D and A can be then obtained by the power-law-regression analysis based on the obtained data. The obtained fitting lines and the power law equations are also presented in Fig. 9, where it shows that the fractal parameters of the surface scanned by the TS is $D = 2.25$ and $A = 0.0206$, which is slightly different than those obtained by the measurements of the laser scanner, $D = 2.21$ and $A = 0.0132$. Figure 9 also shows that the two parallel fitting lines are intercepted with the Y-axis at different positions, which indicates that the parameter D obtained from both methods is almost the same, only the parameter A is slightly different. This is likely due to the lower resolution of the TS method. If the resolution of the TS was increased, the more comparable results might be achieved.

To extend the comparison between these two scanning methods, several cross sections were made at the same locations of the two scanned surfaces of the rep-

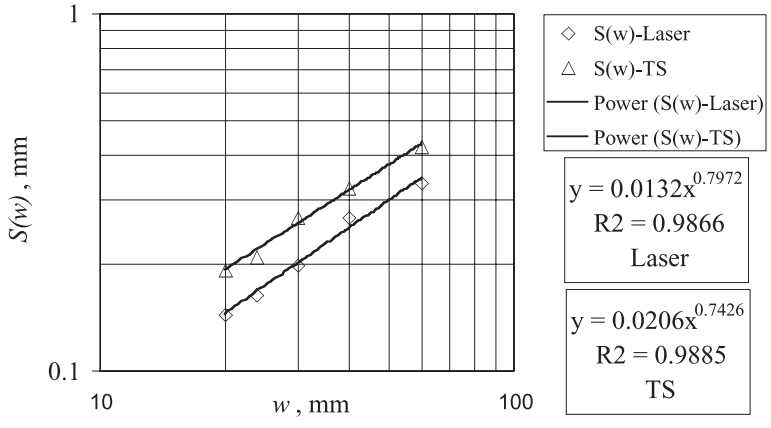

Fig. 9. The power law relationship between $S(w)$ and w for replica surface obtained from 3D-laser scanner and the TS

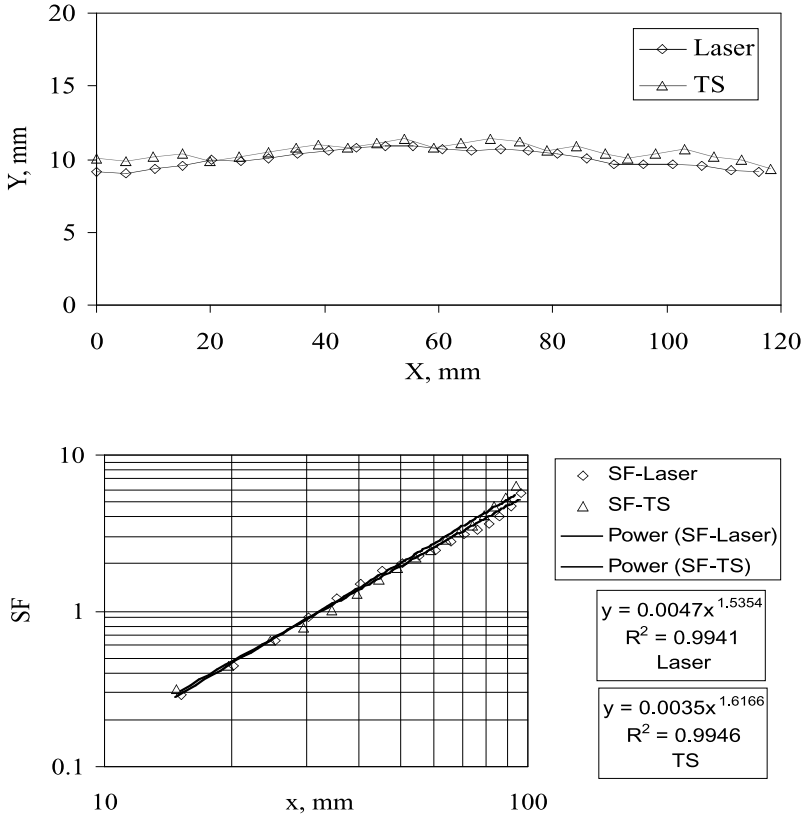

Fig. 10. Cross-sections made from digitised surfaces of replica and their SF values

lica, and then the SF method was applied for roughness analysis. A pair of typical cross-sections and the plotting of SF versus x (horizontal separation) are shown in Fig. 10. It shows that the fractal parameters, D and A, of the cross sections created by both methods are also similar, i.e. $D = 1.19$ and $A = 0.0035$ for the TS method; $D = 1.23$ and $A = 0.0047$ for the laser scanner method.

The above comparable results indicate that the TS method can well quantify the surface roughness for a certain density of the sampling points, and is good for characterizing the primary roughness (larger than 1 mm) of fracture surfaces. The resolution of the TS puts limits to quantify the secondary roughness (less than 1 mm).

5. Scanning of a Large Fracture Surface in the Field

A case study was performed at a road-cut rock face for measuring the undulation of a larger fracture surface in order to validate the applicability of the presented method. The rock face is located along a highway (Stockholm, Sweden). The frac-

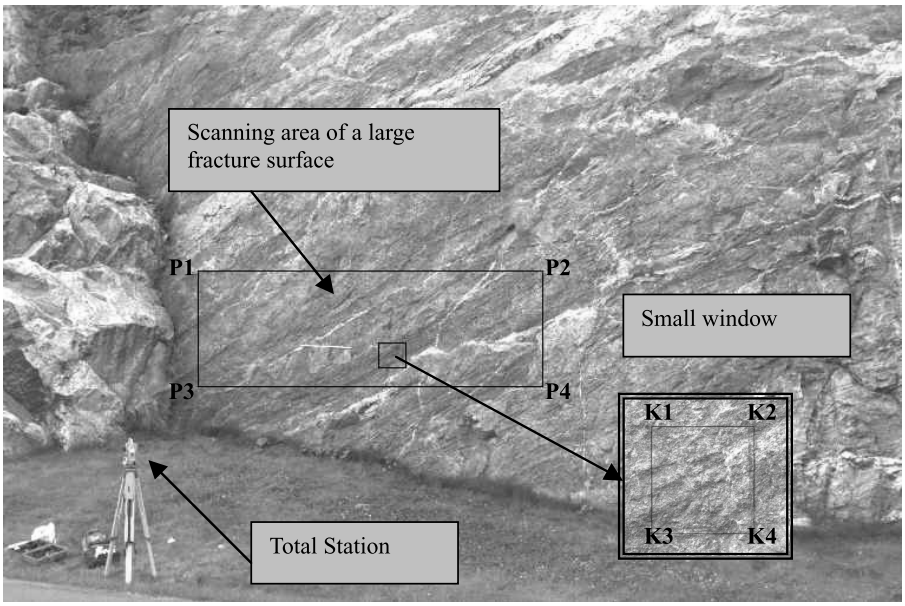

Fig. 11. In-situ scanning of a large fracture surface by the non-reflector TS

ture is cutting through a grayish-red, medium-grained granite rock and belongs to a NW-SE extensional fracture zone. The fracture surface exposed at the rock face is about 20 m × 15 m. A part of this larger fracture surface (about 9 m × 2.5 m) and a small window inside this part (about 20 cm × 20 cm) were scanned by the TS method (see Fig. 11).

A non-reflector TS, Leica TCRM 1102, and the scanning program, Leica TMS PROscan (Leica, 1999), were used for scanning the fracture surface. The TS was positioned at a distance of about 7 m away from the rock face. Before scanning, an oriented local Cartesian co-ordinate system with the known true North was established by using the TS and a compass. The orientation of the fracture surface and the directional features of the fracture roughness in space could be analyzed. Four corner points, P1, P2, P3 and P4, were sequentially measured to define the scanning area of 9 m × 2.5 m in dimension. The sampling interval along the X-direction (e.g. P1–P2) and the Y-direction (e.g. P1–P3) was then defined to be 10 cm for both directions. A small window of 20 cm × 20 cm inside this area was selected to be scanned in detail at 5 mm interval in order to study the scale effect on fracture roughness. The scanning data were first stored in a PCMCIA Flesh memory card in the field, and later downloaded to the PC for data processing. The software Surfacer Imageware was used for roughness analysis. 3-D digital models of the large scanning area and the small window of the fracture surface are shown in Fig. 12.

To analyze the roughness of the large scanning area, a rectangle area of 8 m × 2 m in size was selected. The fractal parameters of the selected surface were

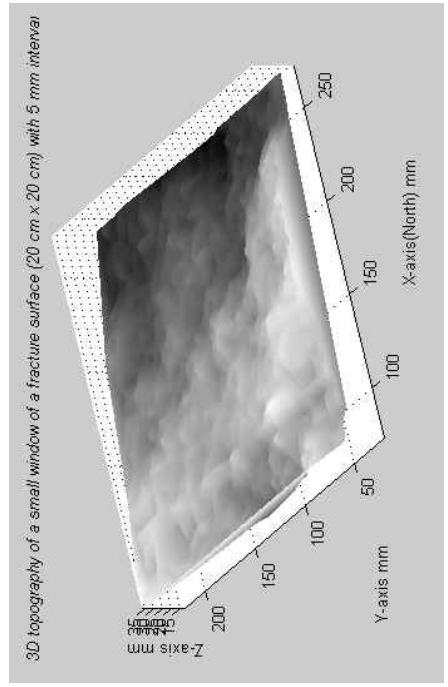

(a) **(b)**

Fig. 12. Digital models of the large scanning area **(a)** and the small window **(b)**

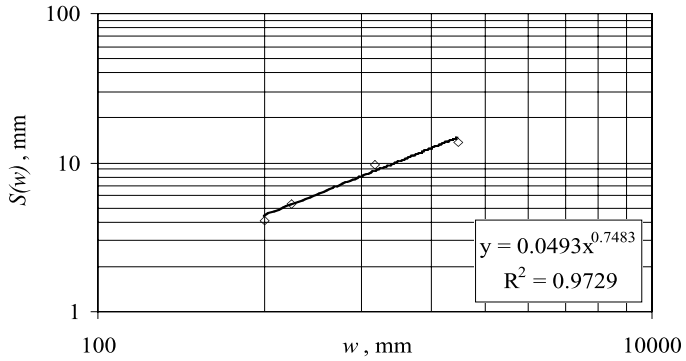

Fig. 13. Standard deviation of reduced asperity height $S(w)$ versus window size w for the rectangular area of the large fracture surface

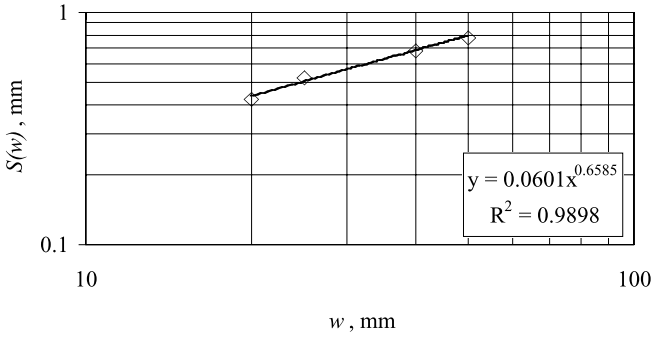

Fig. 14. Relationship of $S(w)$ versus w for the small window surface

calculated by using the RL method. In this case, a series of sampling windows with the size w of 400, 500, 1000 and 2000 mm were chosen. The standard deviations of reduced asperity height $S(w)$ were computed for the series of window sizes w and plotted in a log-log diagram (see Fig. 13). A very good linear relationship was obtained. The roughness of the large sampled surface can be characterized by $D = 2.2517$ and $A = 0.0493$.

Using the same analysis methods, the roughness of the small window inside the scanned surface was quantified. Within the area of 200 mm $\times$ 200 mm, a series of sampling square windows with the defined size w of 20, 25, 40 and 50 mm were chosen. Figure 14 shows the relationship for the standard deviations of reduced asperity height $S(w)$ versus the defined window size w. The fractal parameters of the small window are estimated as $D = 2.3415$ and $A = 0.0601$. The result indicates the existence of a scale effect for the large surface and the small window. The discrepancy is due to different density of sampling points, different position on the fracture surface, and different sizes of the sampling windows.

With the presented method, spatial analysis of fracture roughness is also possible. From the recorded co-ordinates of the points by using the method presented

Table 1. Orientation and roughness of five profiles on the large fracture surface

Cross-section	Trend	Plunge	A	D
Z-1	121°	58°	0.7386	1.4335
Z-2	148°	53°	0.4027	1.3603
Z-3	118°	67°	0.4034	1.3307
Z-4	301°	56°	0.203	1.27875
Z-5	297°	63°	0.4114	1.3529

by Feng et al. (2001), the orientation of the scanned fracture surface is determined to be 027°/65°. The orientation of a profile with a certain roughness property can also be determined, see Table 1.

6. Discussion

The TS is usually used to measure the position of target points in surveying and mapping. However, the non-reflector TS controlled by a special program can also be used as a point-sensor laser scanner to capture the roughness measurements of fracture surfaces automatically and without touching the rock face physically. Therefore, the advantage of the presented method is to characterize the roughness of fracture surfaces at inaccessible and dangerous rock faces.

Since the TS is designed to measure the targets at a long distance, a large fracture surface can be scanned with the TS directly from the rock faces in the field. The areas in different locations and with different sizes on the fracture surface can be scanned with different interval of points. It is well known that fracture roughness is scale dependent, which means that different sizes of samples and different densities of sampling points might result in different roughness for one and the same fracture. By using the TS method, the range of sampling size (up to tens of square meters) of a fracture surface and the interval (from several meters to about 1 mm) of the sampling points can be greatly extended. In addition, small samples can be defined from a large fracture surface, and then be characterized in detail. Therefore, the scale effect and anisotropy of fracture roughness can be efficiently investigated by using the TS method, and both the roughness and the waviness of a large-scale fracture surface can be quantified.

The TS is a tool for control survey in geodesy. It can be used not only for measuring the co-ordinates of target points, but also establishing a local co-ordinate system and linking to a known co-ordinate system if GPS (Global Positioning System) was used. Comparing with other methods, the TS method is particularly useful for spatial analysis of fracture roughness. Therefore, characterization of fracture roughness at field scale becomes possible for rock engineering practice.

Compared with the high accuracy 3-D laser scanner, the primary roughness of fracture surfaces can be accurately measured. However, results of the case study indicated that the secondary roughness of fracture surfaces is impossible to be characterized due to the resolution of the TS. In addition, the scanning speed is not fast enough because of too much mechanic movement of the TS. So, it is time-consuming to scan a large fracture surface with a high density of points.

Measurement accuracy of fracture roughness by using the TS depends upon the surface-related factors, such as inclination angle, surface roughness and reflectance. To obtain accurate measurements of fracture roughness, all factors must be carefully inspected and optimally chosen, and considered in evaluation of the results.

The scanning program used in this study has several drawbacks. For instance, the sampling points are not located exactly in the grid if the area defined by the four corner points are not completely fitted to the defined interval. In addition, each data file can only save less than 1000 points. These drawbacks can be avoided by using other recently-developed programs or by modifying the functions of the used program.

7. Conclusions

The method presented in this paper provides an approach for in-situ non-contact roughness measurement of large-scale fracture surfaces within a maximum distance of several tens of meters from the rock faces. The non-reflector TS controlled by a special program can be taken as a point-sensor laser scanner to measure the roughness of fracture surfaces automatically.

Comparing with the high accuracy 3-D laser scanner, the TS method can accurately measure the primary roughness of fracture surfaces. But the secondary roughness of fracture surfaces can not be detected due to the resolution of the TS.

The scale effect and anisotropy of fracture roughness might be characterized by using TS method. By establishing a known co-ordinate system, both quantitative and spatial analysis of fracture roughness are possible.

The accuracy of the TS depends on not only the measurements of the distance and the angle, but also the surface-related factors, such as inclination angle, roughness of the rock surfaces, reflectance of different material surfaces and distance from the TS to the targets. Therefore, the influence of these factors must be considered when capturing the roughness measurements of fracture surfaces directly from the rock faces.

Acknowledgements

This study was financially supported by Axel and Margaret Ax:son Johnson Foundation, Stockholm, Sweden. The second author would like to thank the Ministry of Science, Research and Technology (MSRT) of the I. R. Iran for financial support. Special thanks are given to Åke Bollö, Leica Geosystem AB, Stockholm and Sven Vejder, SBG AB, Stockholm for their kind help in using the TS instrument and the scanning programs. Per Delin, Division of Soil and Rock Mechanics, Royal Institute of Technology, Sweden, is acknowledged for his help to make the replica.

References

Barton, N., Choubey, V. (1977): The shear strength of rock joints in theory and practice. Rock Mechanics 10, 1–54.

Berry, M. V., Lewis, Z. V. (1980): On the Weierstrass-Mandelbrot fractal function. R. Soc. London Proc. Ser. A. 370, 459–484.

Brown, S. R., Scholz, C. H. (1985): Broad bandwidth study of the topography of natural rock surfaces. J. Geophys. Res. 90 (B14), 12575–12582.

Bulut, F., Tüdes, S. (1996): Determination of discontinuity traces on inaccessible rock slopes using electronic tacheometer: an example from the Ikisdere (Rize) Region, Turkey. Engng. Geol. 44, 229–233.

Fan, H. (1997): Theory of errors and least squares adjustment. Lecture Notes, Division of Geodesy, Department of Geodesy and Photogrammetry, Royal Institute of Technology, Stockholm, Sweden.

Fardin, N., Stephansson, O., Jing, L. (2001): The scale dependence of rock joint surface roughness. Int. J. Rock Mech. Min. Sci. 38, 659–669.

Fecker, E., Rengers, N. (1971): Measurement of large scale roughness of rock planes by means of profilograph and geological compass. Rock fracture. In: Proc., Symp. Int. Soc. Rock Mech., Nancy, France, 1–18.

Feng, Q., Sjögren, P., Stephansson, O., Jing, L. (2001): Measuring fracture orientation at exposed rock faces by using a non-reflector total station. Engng. Geol. 59, 133–146.

Galante, G., Piacentini, M., Ruisi, V. F. (1991): Surface roughness detection by image processing tool. Wear 148 (2), 211–220.

Grasselli, G., Egger, P. (2000): 3D surface characterization for the prediction of the shear strength of rough joints. In: Proc., EUROCK 2000 14. Nationales Symposium für Felsmechanik und Tunnelbau, Aachen, Germany, 281–286.

Imageware, Inc. (1999): Surfacer User's Guide, Ver. 10.0. Imageware, Inc., Ann Arbor, Michigan, USA.

Kavanagh, B. F., Glenn Bird, S. J. (1992): Surveying principles and applications, 3rd edn. Prentice Hall, Englewood Cliffs, New Jersey, USA.

Lanaro, F., Jing, L., Stephansson, O. (1998): 3D-laser measurements and representation of roughness of rock fractures. In: Proc., Mechanics of Jointed and Faulted Rock, Vienna, A.A. Balkema, Rotterdam, 185–189.

Leica (1998): Manual of Leica TCRM 1102.

Leica (1999): Manual of Leica TMS PROscan.

Maerz, N. H., Franklin, J. A., Bennett, C. P. (1990): Joint roughness measurement using shadow profilometry. Int. J. Rock Mech. Min. Sci. Geomech. Abstr. 27, 329–343.

Mandelbrot, B. B. (1967): How long is the coast line of Britain? Statistical self-similarity and fractal dimension. Science 155, 636–638.

Mandelbrot, B. B. (1983): The fractal geometry of nature. W. H. Freeman, New York.

Malinverno, A. (1990): A simple method to estimate the fractal dimension of a self affine series. Geophys. Res. Lett. 17, 1953–1956.

Matsushita, M., Ouchi, S. (1989): On the self affinity of various curves. Physica D 38, 246–251.

Moffitt, F. H., Rossler, J. D. (1998): Surveying, 10. edn. Addison Wesley Longman, Inc., Menlo Park, California, USA.

Odling, N. E. (1994): Natural fracture profiles, fractal dimension and joint roughness coefficient. Rock Mech. Rock. Engng. 27, 135–153.

Orey, S. (1970): Gaussian simple functions and Hausdorff dimension of level crossing. Z. Wahrscheinlichkeitstheor. Verw. Gebiete 1970.

Piggott, A. R., Elsworth, D. (1995): A comparison of methods of characterising fracture surface roughness. In: Fractured and jointed rock masses. Balkema, Rotterdam, 471–477.

Poon, C. Y., Sayles, R. S., Jones, T. A. (1992): Surface measurement and fractal characterization of naturally fractured rocks. J. Phys. D Appl. Phys. 25, 1269–1275.

Rasouli, V., Harrison, J. P. (2000): Scale effect, anisotropy and directionality of discontinuity surface roughness. In: Proc., EUROCK 2000 14. Nationales Symposium für Felsmechanik und Tunnelbau, Aachen, Germany, 751–756.

Roko, R. O., Daemen, J. J. K., Myers, D. E. (1997): Variogram characterization of joint surface morphology and asperity deformation during shearing. Int. J. Rock. Mech. Min. Sci. 34 (1), 71–84.

Sayles, R. S., Thomas, T. R. (1977): The spatial representation of surface roughness by means of the structure function: a practical alternative to correlation. Wear 42, 263–276.

Shukla, R. P., Perera, G. M., Venkateswarlu, P., George, M. C. (1991): Interferometric techniques for correction of sample tilt in the sommergen profilometer for surface roughness studies. Opt. Laser Technol. 23 (2), 98–104.

Svenska Byggnads Geodesi (SBG) AB (1999): Manual of Geo and GeoPad. Solna, Sweden.

Voss, R. (1988): Fractals in nature. In: Peitgen, H., Saupe, D. (eds.), The science of fractal images. Springer, Wien New York, 21–69.

Weissbach, G. (1978): A new method for the determination of the roughness of rock joints in the laboratory. Int. J. Rock Mech. Min. Sci. Geomech. Abstr. 15, 131–133.

Wickens, E. H., Barton, N. R. (1971): Application of photogrammetry to the stability of excavated rock slopes. Photogram. Record 7, 46–54.

Xie, H. (1993): Fractals in rock mechanics. A.A. Balkema, Rotterdam.

Yilbas, Z., Hashmi, M. S. J. (1998): An optical method and neural network for surface roughness measurement. Optics and Lasers in Engineering 29, 1–15.

Yilbas, B. S., Danisman, K., Yilmaz, M., Yilbas, Z. (1987): The development of the computer controlled electro-fiber system for surface roughness measurements. Metrology Optoelectronic Systems, SPIE 776, 55–58.

Authors' address: Quanhong Feng, Berg Bygg Konsult (BBK) AB, Ankdammsgatan 20, SE-171 43 Solna, Sweden; e-mail: feng@bergbyggkonsult.se